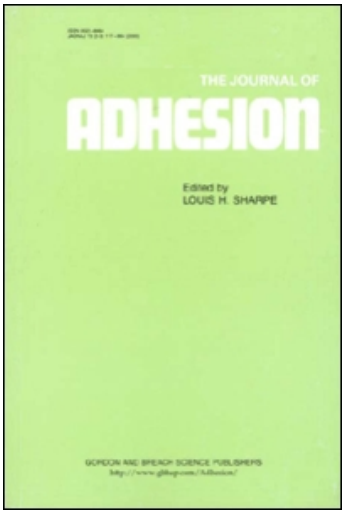

The Journal of Adhesion
Publication details, including instructions for authors and subscription information:
http://www.informaworld.com/smpp/title~content=t713453635

Fatigue Failure Criterion of Adhesively-Bonded Joints Under Combined Stress Conditions

Makoto Imanaka[a]; Takayoshi Iwata[b]
[a] Osaka University of Education, Kashiwara City, Japan [b] Technical Research & Development Dept, Toyoda Gosei Co Ltd, Inazawa City, Japan

To cite this Article Imanaka, Makoto and Iwata, Takayoshi(1996) 'Fatigue Failure Criterion of Adhesively-Bonded Joints Under Combined Stress Conditions', The Journal of Adhesion, 59: 1, 111 — 126
To link to this Article: DOI: 10.1080/00218469608011081
URL: http://dx.doi.org/10.1080/00218469608011081

J. Adhesion, 1996, Vol. 59, pp. 111–126
Reprints available directly from the publisher
Photocopying permitted by license only

Fatigue Failure Criterion of Adhesively-Bonded Joints Under Combined Stress Conditions*

MAKOTO IMANAKA**

Osaka University of Education,
Asahigaoka, Kashiwara City, Osaka Pref. 582, Japan

and

TAKAYOSHI IWATA

Technical Research & Development Dept., Toyoda Gosei Co., Ltd.
Kitajima-cho, Inazawa City, Aichi Pref. 492, Japan

(In final form January 19, 1996)

A study was conducted to investigate fatigue failure criteria for adhesively-bonded joints under combined stress conditions. Two types of adhesively-bonded joint specimens were used: the scarf joint and the butterfly-type butt joint. Both types of joints have considerably uniform combined stress distributions in the adhesive layer. Furthermore, the stress distributions of these joints were analyzed by a finite element method. The results showed that the maximum principal, the von Mises equivalent and the maximum shear stresses in the uniform stress region of the adhesive layer at the endurance limit are correlated with the principal stress ratio.

KEY WORDS: Fatigue testing; combined stress conditions; scarf joint; butterfly-type butt joint; stress analysis; stress distribution; finite element analysis; maximum principal stress; von Mises equivalent stress; maximum shear stress; endurance limit.

1. INTRODUCTION

Most adhesively-bonded joints have concentrated multiple stress components, *i.e.* peel, shear and axial stresses in the adhesive layer. Hence, to predict the strength of adhesive joints with a high degree of accuracy, a knowledge of stress distribution in the adhesive layer must be coupled with a suitable failure criterion obtained from standard adhesive joints with uniformly distributed multiple stress components in the adhesive layer. However, it is very difficult to obtain completely uniform stress distributions in the adhesive layer because of stress singularity in different material wedges with an interlayer.

*Presented at the International Adhesion Symposium, *IAS'94 Japan*, at the 30th Anniversary Meeting of the Adhesion Society of Japan, Yokohama, Japan, November 6–10, 1994.

**Corresponding author.

Two types of adhesive-bonded joints have considerably uniform combined stress distributions in the adhesive layer under uniaxial loading conditions: adhesive-bonded scarf and butterfly-type butt joints. Scarf joints have quite uniform normal and shear stresses, and their combination ratio can be varied by changing scarf angle. Hence, there have been numerous studies on scarf joints since stress distributions in this type of joint were investigated by Lubkin[1]. Recently, static strength characteristics of scarf joints have been investigated by Suzuki[2-4], David *et al.*[5] and Kyogoku *et al*[6]. However, it is difficult to obtain conditions where the shear stress is dominant or is the sole stress. For pure shear and combined stress conditions, Arcan *et al.* proposed a testing method for homogeneous and bonded specimens under unidirectional loading conditions[7], which has been applied for measurement of shear strength and Mode II fracture toughness of several materials[8-11].

In this study, to obtain fatigue failure criteria under combined stress conditions, fatigue tests were conducted for two kinds of adhesive-bonded specimens; scarf joints and butterfly-type butt joints, as proposed by Arcan[7], where both joints have considerably uniform combined stress distributions in the adhesive layer. In addition, the stress distributions in these joints were analyzed by a finite element method. Our results confirmed that the maximum principal, the von Mises equivalent and the maximum shear stresses in the uniform stress region of the adhesive layer at the endurance limit are correlated with the principal stress ratio.

2. EXPERIMENTAL METHOD AND ADHESIVE BONDED JOINT SPECIMENS

The adherends for butt, scarf and butterfly-type butt joints were 0.5%C structural carbon steel (JIS. S55C). The adhesive was a thermosetting structural epoxy adhesive (EA9432NA: Toyada Gosei Co. Ltd., Japan).

Details of the butt and scarf joints are shown in Figure 1. The scarf angle was varied between six values, *i.e.* 30°, 33.75°, 45°, 60°, 75° and 90° (butt joint). The width of the adherend varied with scarf angle to maintain a constant adhesive area of 190 mm^2.

The butterfly-type butt joint and its loading frame are shown in Figure 2. The butterfly-type butt joint specimen was assembled into the loading frame by six pins, and the loading frame was fastened with two pins into the fatigue testing machine. The ratio of normal stress to shear stress can be varied by changing the location of upper and lower fixed pins in the loading frame. In this study, fatigue tests were

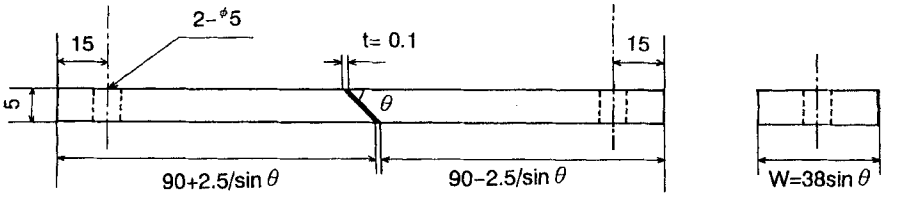

FIGURE 1 Shape and sizes of the butt and scarf joints.

conducted with inclination angles of $\theta = 0°$ and $\theta = 11.25°$, where the center of the adhesive layer lay on the loading line and deviated from the loading line by 11.25°, respectively.

Adhesively-bonded specimens were prepared as follows: The bonding surfaces of adherends were polished with emery paper of grade 180 mesh under dry condition. Then, the specimens were degreased with acetone in an ultrasonic bath. The adhesive layer thicknesses of the specimens were set up to 0.1mm using an adhesion jig incorporating a micrometerhead. The adhesive joints were then cured in an oven at 140°C for 1.5hr and allowed to cool in the oven. Joint specimens thus obtained were allowed to stand for a day at room temperature before being subjected to fatigue tests.

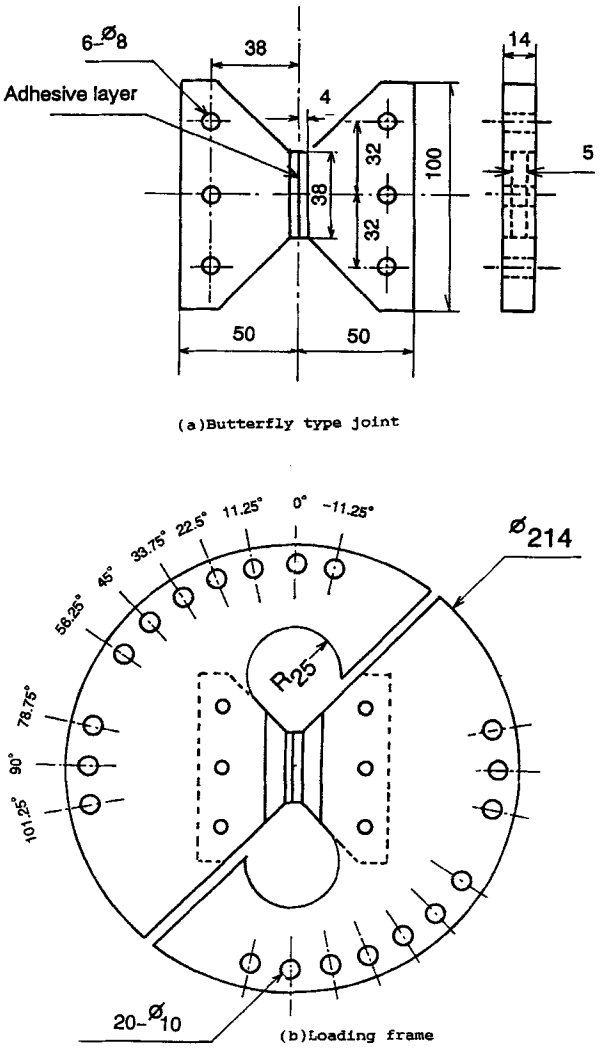

FIGURE 2 Shape and sizes of the butterfly-type joint and the loading frame.

Cyclic tensile fatigue tests were conducted with an electro-hydraulic type closed loop fatigue testing machine under the condition of stress ratio $R = 0.1$ and loading frequency of 30 Hz.

3. STRESS ANALYSIS

The stress distributions of these joints were analyzed by a two-dimensional finite element method, where a plane strain condition was assumed. The material properties used in this analysis were as follows: Young's modulus and Poisson's ratio of the adhesive and of the adherend were 4.3 GPa and 0.319, 200 GPa and 0.291, respectively.

Figure 3 shows the boundary conditions and an example of the mesh pattern near the adhesive layer at the free end of the butt and scarf joints. As shown in this figure, one side of the joint was fixed and uniform displacement was applied to the other side. The boundary conditions and mesh pattern of the butterfly-type butt joint are indicated in Figure 4. As shown in this figure, one point of the loading frame was fixed and a concentrated load, P, was applied to, the other side. In this study, stress analysis was conducted with $\theta = 0°$ and 11.25°. In Figures 3 and 4, s and n indicate

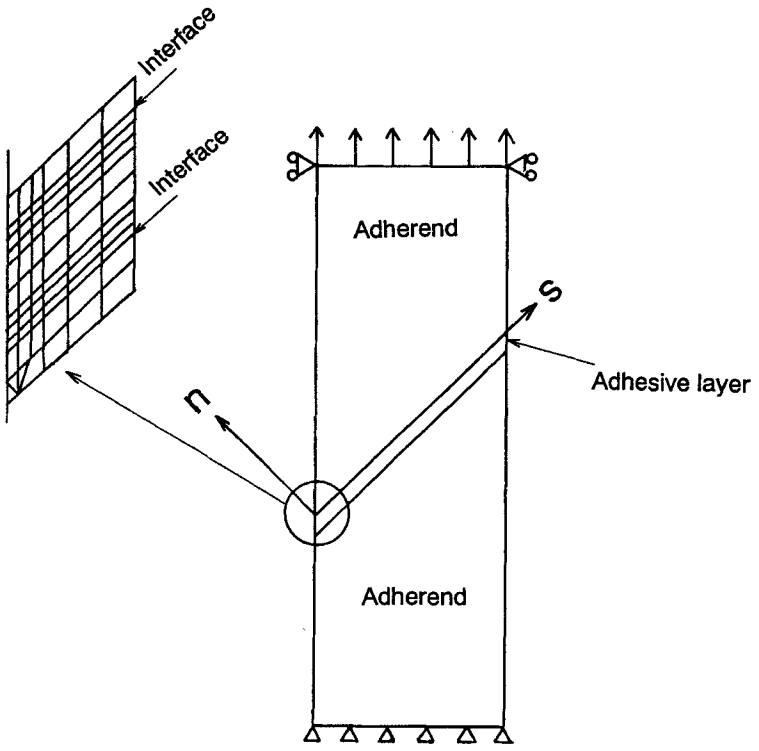

FIGURE 3 Boundary conditions of the butt and scarf joints, and an example of the mesh pattern near the free end of the adhesive layer.

the direction perpendicular to the adhesive/adherend interface and normal to the interface, respectively. Hereafter, we refer to these directions as s and n directions, respectively.

Stress distributions of the adhesive/adherend interface are shown in Figure 5(a)–(e) for the normal stress, σ_{nn}, the shear stress, τ_{ns}, the maximum principal stress, σ_1, the von Mises equivalent stress, σ_{mie} and the maximum shear stress, τ_{max}, respectively, where the locations of the stress distribution are Gaussian integration points within the adhesive layer nearest to the adhesive/adherend interface. In this figure, the value on the ordinate indicates the distance from the free end of the adhesive layer where the maximum stress appears, and the value on the abscissa is normalized with respect to the average tensile stress of the adherend plate.

Figure 5 shows that all stress components arise near the free end of the adhesive layer, whereas in the inner range beyond a point several times as long as the adhesive layer thickness removed from the free end, all the stress components have nearly uniform values.

When adherends are regarded as rigid bodies and under a plane strain condition, σ_{nn}, τ_{ns} and σ_2 representing tensile stress in the width direction are expressed by the following equations[2].

$$\sigma_{nn} = \sigma_a \sin^2\theta \tag{1}$$

$$\tau_{ns} = \sigma_a \sin\theta\cos\theta \tag{2}$$

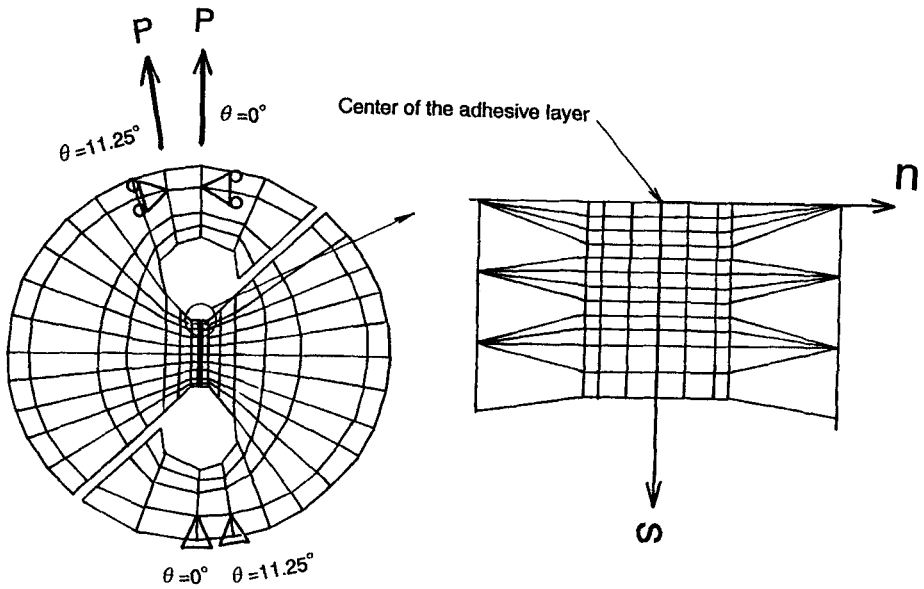

FIGURE 4 The element of butterfly-type joint in the FEM analysis and boundary conditions.

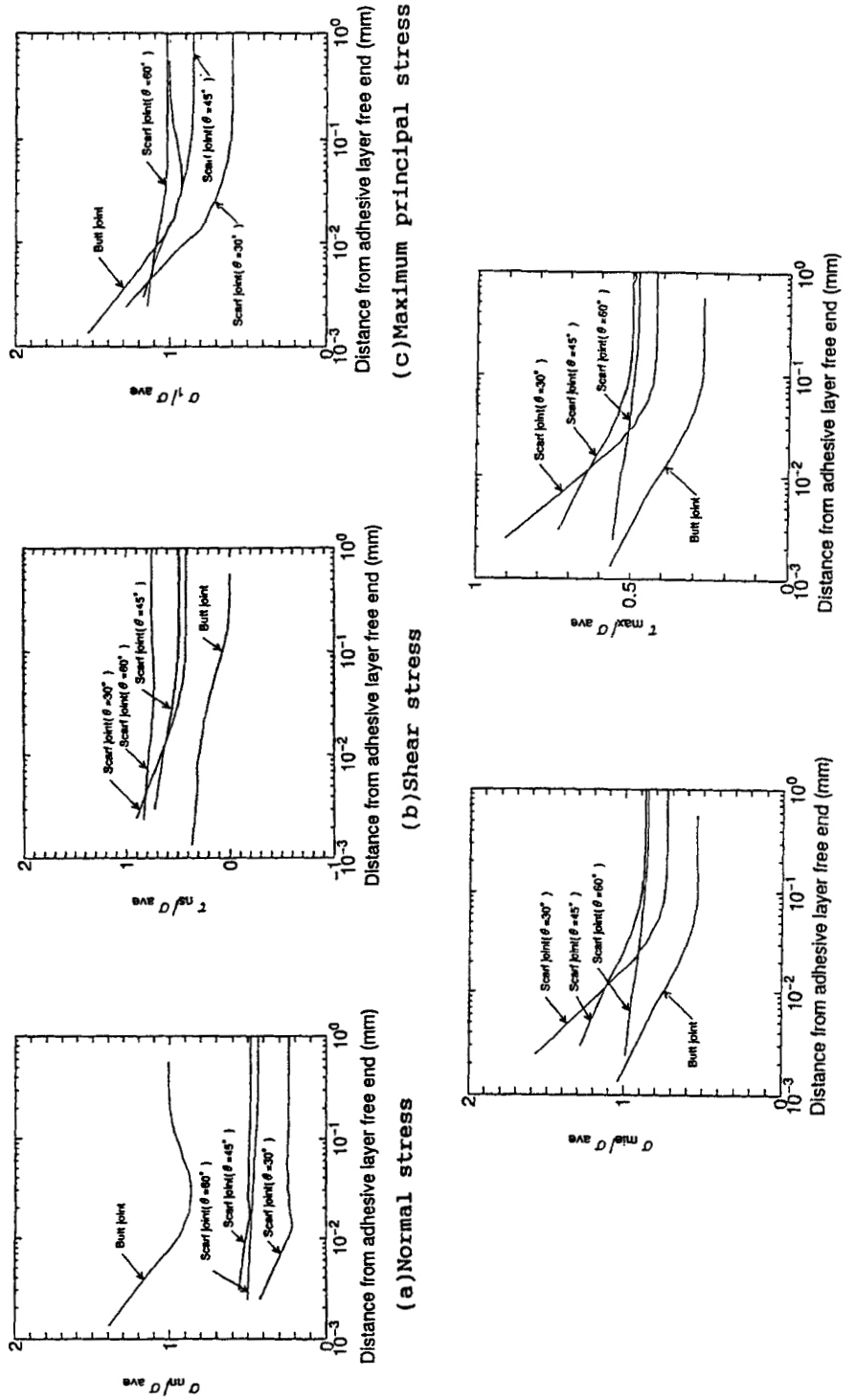

FIGURE 5 Stress distributions along adhesive/adherend interfaces of butt and scarf joints in the vicinity of the free end of the adhesive where the maximum stress appears.

$$\sigma_z = \sigma_s = \frac{v_a}{1 - v_a}\sigma_a \tag{3}$$

where σ_a and v_a are average tensile stress of the adherend and Poission's ratio of the adhesive layer, respectively.

Furthermore, Eqs. (1)–(3) give the maximum, the medium and the minimum principal stresses as the following equations[2].

$$\sigma_1 = \frac{1}{2}(\sigma_s + \sigma_{nn} + \sqrt{(\sigma_s - \sigma_{nn})^2 4\tau_{ns}^2} \tag{4}$$

$$\sigma_2 = \sigma_s = \sigma_z \tag{5}$$

$$\sigma_3 = \frac{1}{2}(\sigma_s + \sigma_{nn} - \sqrt{(\sigma_s - \sigma_{nn})^2 + 4\tau_{ns}^2}) \tag{6}$$

It was confirmed that the values of σ_{nn}, τ_{ns}, σ_1, σ_{mie} and τ_{max} in the uniform stress region in Figure 6 coincide almost exactly with the values calculated by Eqs. (1)–(6).

When the scarf angle, θ, agress with the value derived by Eq. (7) and the plane strain condition is assumed, Lubkin and Suzuki showed that the stress singularity at the free end of the adhesive layer disappears and an entirely uniform stress distribution is obtained[1,2].

$$\tan^2\theta = \frac{\mu - 1}{\dfrac{\mu v_s}{1 - v_s} - \dfrac{v_a}{1 - v_a}} \tag{7}$$

$$\text{where } \mu = \frac{(1 - v_s^2) E_a}{(1 - v_a^2) E_s}$$

Here, E_a and E_s are young's moduli of the adhesive layer and adherend, respectively, and v_s is the Poission's ratio of the adherend. By substituting the material constants in Eq. (7), the angle $\theta = 55.57°$ at which stress singularity disappears is obtained. The scarf angle $\theta = 60°$ is closest to this angle in the scarf joints as shown in Figure 5. Therefore, the scarf joint of $\theta = 60°$ gives the most gentle stress gradient near the free end of the adhesive layer in scarf joints.

Figures 6 and 7 show the stress distributions along the adhesive/adherend interface for the butterfly-type butt joints with $\theta = 0°$ and 11.25°, respectively. In Figure 6, values on the ordinate are normalized by the average shear stress, τ_{ave}, obtained by dividing applied load by bonding area. On the other hand, the values on the ordinate in Figure 7 are normalized by the average tensile stress obtained by dividing applied load by the area obtained by projecting the adhesive area onto the surface normal to the loading axis.

Figure 6(a) indicates that σ_{nn} increases to infinity and τ_{ns} decreases to zero at the free end. However, σ_{nn} and τ_{ns} approximate to zero and unity, respectively, except near the free end. In Figure 6 (b), σ_1, σ_{mie} and τ_{max} have almost uniform values in the middle of the adhesive layer, and decrease closer to the end except in the vicinity of the free end.

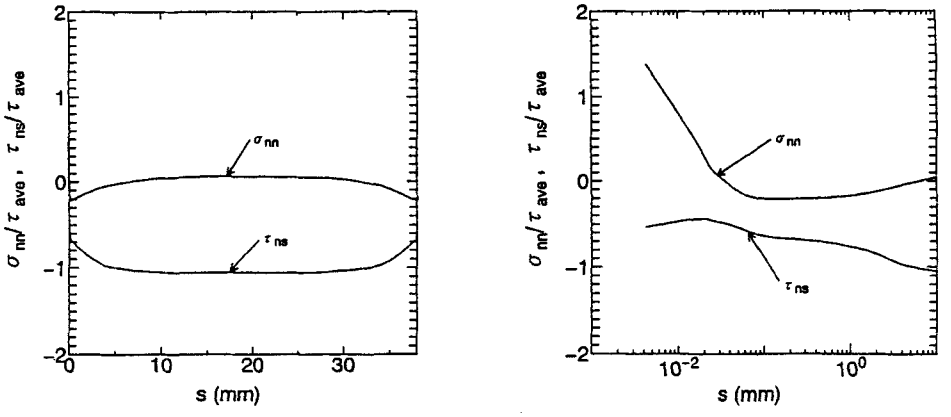

(a)Normal and shear stresses

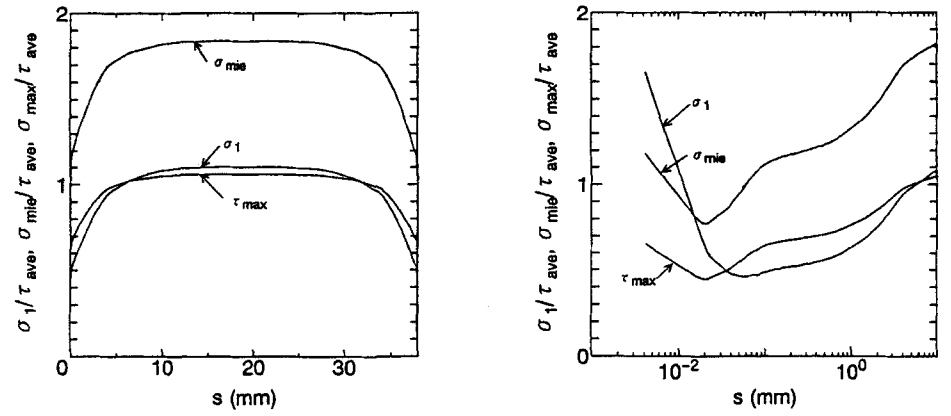

(b)Maximum principal, Mises equivalent and maximum shear stresses

FIGURE 6 Stress distributions along adhesive/adherend interface of the butterfly-type joint in the adhesive layer ($\theta = 0°$).

For the butterfly-type butt joint with $\theta = 11.25°$, it can be seen from Figure 7 that all stress components are reasonably uniform, although σ_{nn}, σ_1, σ_{mie} and τ_{max} rise sharply near the edge and show maximum values in the middle of the joints except near both free ends.

Generally, negative and positive hydrostatic pressures make most polymeric materials brittle and ductile, respectively[12]. Therefore, when evaluating adhesive strength under combined stress conditions, the effects of hydrostatic pressure, *i.e.* stress multiaxiality, should be considered. To investigate the multiaxiality in the adhesive layer, principal stress ratios in the adhesive layer of the butt, scarf and butterfly-type joints are shown in Figure 8(a) and (b). Figure 8 (a) indicates the

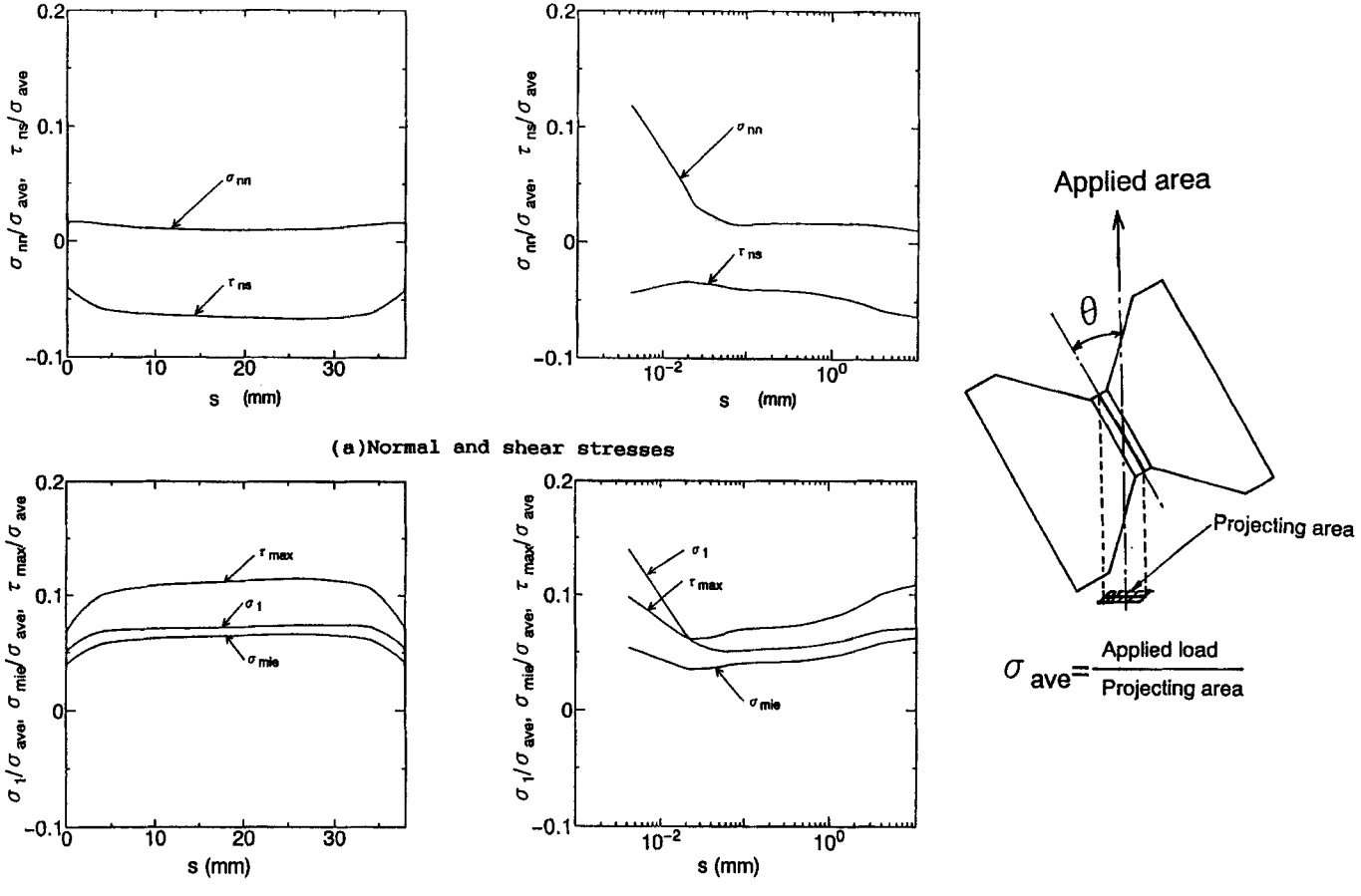

FIGURE 7 Stress distributions along adhesive/adherend interface of the butterfly-type joint in the adhesive layer (θ = 11.25°).

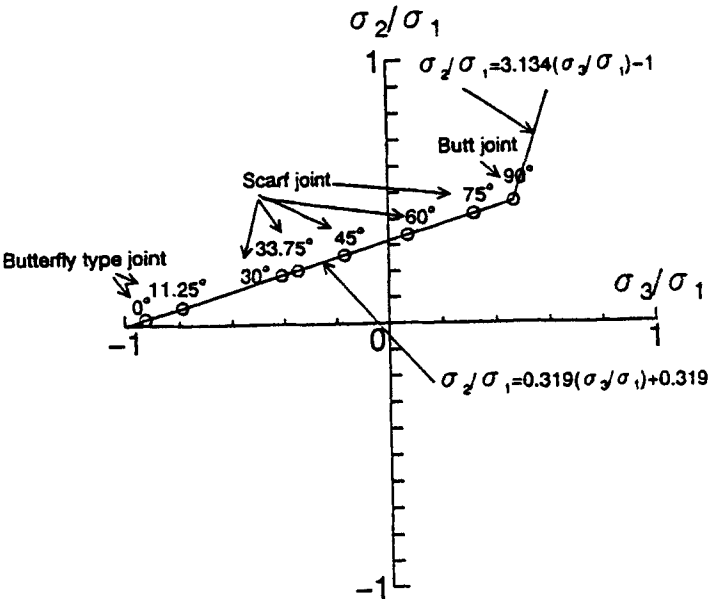

(a)Principal stress ratios in uniform stress regions adhesive layer

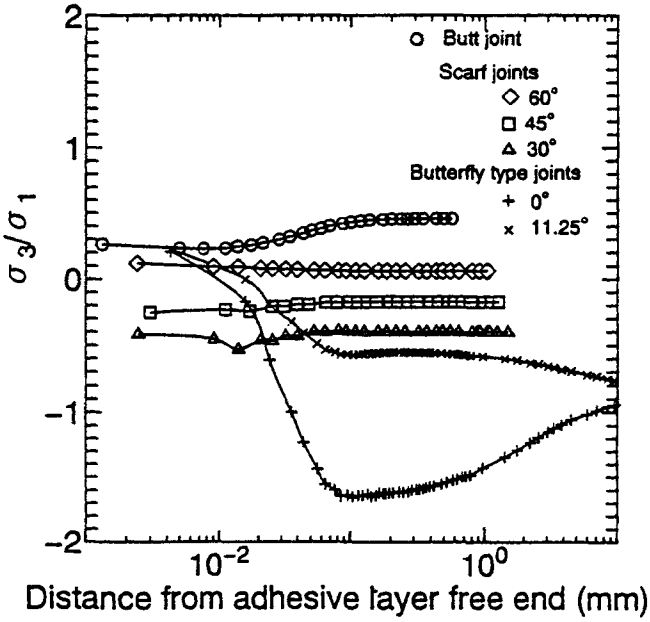

(b)Distributions of principal stress ratios

FIGURE 8 Principal stress ratios of butt, scarf and butterfly-type joints.

principal stress ratios in a uniform stress region, where values on the ordinte and abscissa indicate the ratios of the medium principal stress, σ_2, to the maximum principal stress, σ_1, and of the minimum principal stress, σ_3, to the maximum principal stress, σ_1, respectively.

Under the plane strain condition, the principal stress in the width direction, σ_z, can be represented as

$$\sigma_z = \nu_a(\sigma + \alpha\sigma) \tag{8}$$

where the maximum principal stress is σ, and $\alpha\sigma$ ($\alpha < 1$) is the medium or the minimum principal stress.

When comparing $\alpha\sigma$ with σ_z, the following inequalities are obtained.

$$\alpha \leqslant \frac{\nu_a}{1-\nu_a}, \quad \text{if} \quad \sigma_z \geqslant \alpha\sigma$$

$$\alpha > \frac{\nu_a}{1-\nu_a}, \quad \text{if} \quad \sigma_z < \alpha\sigma \tag{9}$$

Therefore, the following linear relations are given and shown in Figure 8 (a).

$$\frac{\sigma_2}{\sigma_1} = \nu_a + \nu_a \frac{\sigma_3}{\sigma_1} \quad \text{if} \quad \frac{\sigma_3}{\sigma_1} \leqslant \frac{\nu_a}{1-\nu_a} \tag{10-a}$$

$$\frac{\sigma_2}{\sigma_1} = \frac{1}{\nu_a}\left(\frac{\sigma_3}{\sigma_1}\right) - 1 \quad \text{if} \quad \frac{\sigma_3}{\sigma_1} > \frac{\nu_a}{1-\nu_a} \tag{10-b}$$

Hence, if plane strain is assumed, it is confirmed from Eqs. (10-a and -b) that the multiaxial stress condition can be defined by only one parameter, *i.e.* σ_3/σ_1 or σ_2/σ_1. As the principal stress ratios, σ_3/σ_1, of uniform stress ranges of the butt, scarf and butterfly type joints are less than $\nu_a/(1-\nu_a)$, these principal stress ratios agree with the linear relation in Eq. (10-a).

Furthermore, Figure 8(a) shows that when $\sigma_3/\sigma_1 > 0$ ($\theta > 55.5°$), all principal stress components are positive, where polymeric materials exhibit the most brittle characteristics, and that σ_1 and σ_2 are positive and σ_3 is negative in the region of $-1 < \sigma_3/\sigma_1 < 0$. In addition, Figure 8(a) shows that σ_3/σ_1 and σ_2/σ_1 of the butterfly-type butt joints with $\theta = 0°$ are nearly equal to -1 and 0, respectively. This indicates that a nearly-pure shear stress condition is obtained in the uniform stress resion of the butterfly-type butt joint with $\theta = 0°$.

The external hydrostatic pressure, p, can be obtained as follows:

$$p = \frac{(\sigma_1 + \sigma_2 + \sigma_3)}{3} = \sigma_1\left(\frac{\sigma_3}{\sigma_1} + 1\right)(1 + \nu_a) \tag{11}$$

where $\sigma_1 > 0$ and $\sigma_3/\sigma_1 > -1$ for butt, scarf and butterfly-type joints; hence, $p > 0$ for these joints, and p increases with increasing σ_3/σ_1.

Figure 8 (b) shows the distribution of σ_3/σ_1 along the adhesive/adherend interface. This figure indicates that the σ_3/σ_1 ratios of the butt joint decrease gently closer to the end of the free surface, and those of scarf joints whose scarf angles are 30°, 45° and 60° are nearly uniform. However, σ_3/σ_1 ratios of butterfly-type joints with

$\theta = 0°$ and 11.25° decrease rapidly with increasing distance from the end of the free surface; especially, the σ_3/σ_1 ratio of the scarf joint with $\theta = 0°$ has a minimum value near the free end in the joints, and then approaches the fixed value.

4. RESULTS OF FATIGUE TESTS AND DISCUSSION

Figure 9 shows the S-N relationships of the butt and scarf joints. Values on the ordinate indicate the averaged axial stress range of the adherend. Although the adhesive area is constant irrespective of the scarf angle, this figure shows that fatigue strength increase with decreasing scarf angle. For the butterfly-type joint, averaged axial stress is not suitable to arrange S-N relationships. Hence, as shown in Figure 10, load range was used to arrange the S-N relationships of butterfly-type joints with $\theta = 0°$ and 11.25°. Figure 10 indicates that the fatigue strength of the butterfly-type joint with $\theta = 11.25°$ under combined normal and shear stresses is lower than that of the joint with $\theta = 0°$.

To indicate endurance limits of these joints in the same plane, Figure 11 shows the stress conditions at the endurance limit in $\sigma_{nn} - \tau_{ns}$ stress space, where stresses at the endurance limit in the uniform stress region decompose into normal stress, σ_{nn}, and shear stress, τ_{ns}. In this figure, the estimated curves based on the maximum principal, the von Mises equivalent and the maximum shear stresses are also indicated, where critical values are assumed to be those of the butt joint. Figure 11 shows that estimated values based on the maximum principal stress agree with experimental data in the region of $60° \leqslant \theta \leqslant 90°$; however, they underestimate the

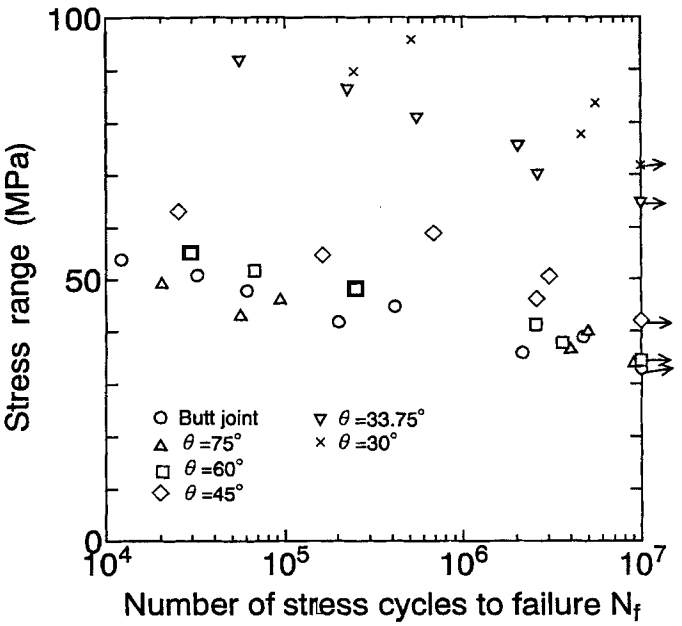

FIGURE 9 S-N relationships of butt and scarf joints with various scarf angles.

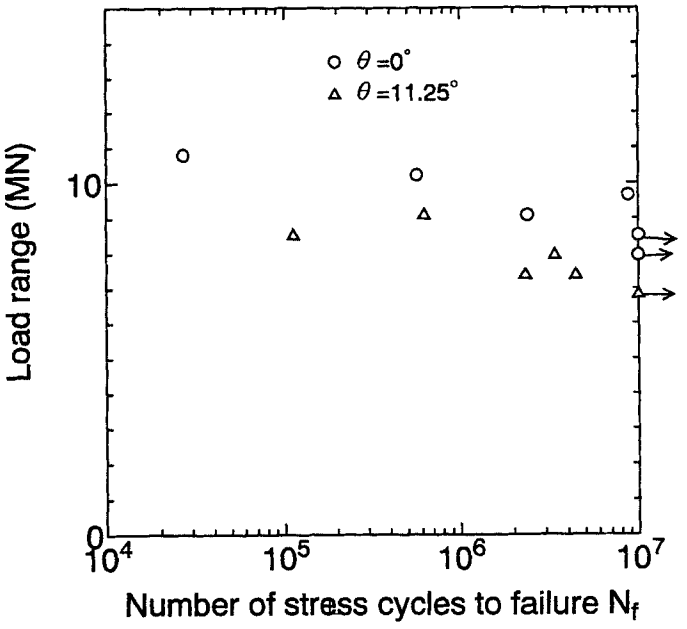

FIGURE 10 S-N relationships of butterfly-type joints.

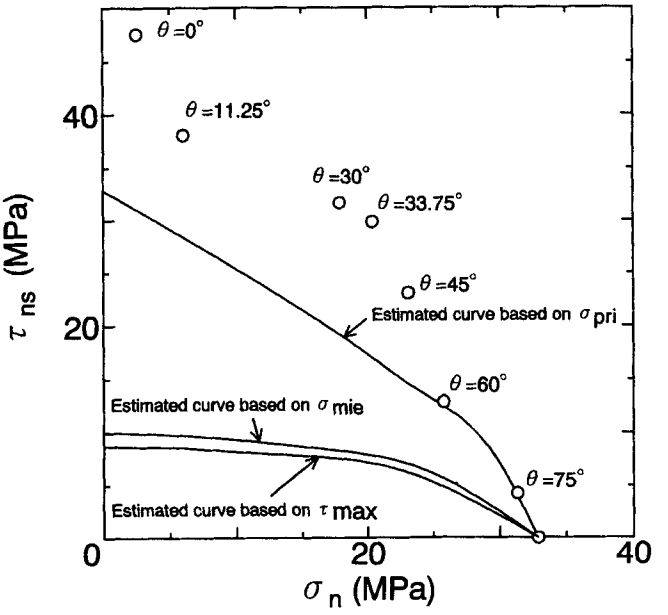

FIGURE 11 Fatigue failure loci under combined stress conditions.

experimental data in the range of $\theta \leqslant 45°$. This figure also indicates that both the estimated values based on the von Mises equivalent and the maximum shear stresses completely disagree with the experimental data. Therefore, the maximum principal, the Von Mises equivalent and the maximum shear stresses are not adequate as criteria for estimating endurance limits of these adhesive joints. These values are expected to depend on multiaxiality of stresses in the adhesive layer.

Figure 12 shows the relationship between the principal stress ratio and the endurance limt, where the value taken on the abscissa is the ratio of σ_3/σ_1 in the uniform stress region of the adhesive layer and the ordiante indicates the maximum principal, the von Mises equivalent and the maximum shear stresses in the uniform stress region at the endurance limit. This figure indicates that good linear relationships between endurance limit and principal stress ratio are obtained irrespective of the kind of stress, and that all kinds of stresses at the endurance limit decrease with increasing principal stress ratio σ_3/σ_1, where the von Mises equivalent and the maximum shear stresses decrease rapidly. The experimental linear equations obtained by least squares analysis are also indicated in this figure, where coefficients of correlation based on the maximum principal, the von Mises equivalent and the maximum shear stresses were 0.906, 0.98 and 0.97, respectively. This indicates that the von Mises equivalent and the maximum shear stresses at the endurance limit are more sensitive to the principal stress ratio than the maximum principal stress. However, the experimental equations based on equivalent von Mises and maximum shear stresses enable us to estimate the endurance limit with slightly higher accuracy than those based on the maximum principal stress.

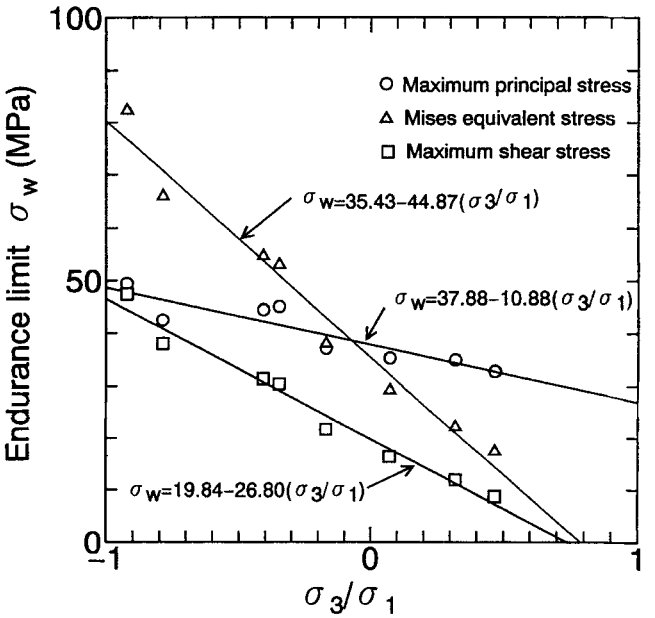

FIGURE 12 Effect of the principal stress ratio on the endurance limit.

CONCLUSIONS

To obtain fatigue failure criteria under combined stress conditions, fatigue tests were conducted for two kinds of adhesively-bonded specimens: scarf joints and butterfly-type butt joints. Furthermore, the stress distributions in these joints were analyzed by a finite element method. To obtain fatigue failure criteria under combined stress conditions, the relationship between the principal stress ratio and fatigue strength of adhesive joints were discussed. Major results obtained in this study are summarized as follows:

(1) All stress components of the butt and scarf joints arise near the free end of the adhesive layer, whereas these stress components have nearly uniform values in the inner range beyond a point several times the adhesive layer thickness away from the free end.
(2) For butterfly-type butt joints with $\theta = 0°$ and 11.25°, σ_1, σ_{mie} and τ_{max} take the maximum values in the middle of the joints except near both free ends.
(3) As a plane strain condition is assumed in this analysis, combined stress conditions of the butt, scarf and butterfly-type joints can be expressed in one linear equation in $\sigma_3/\sigma_1 - \sigma_2/\sigma_1$ space. Furthermore, σ_3/σ_1 of the butt and scarf joints vary slightly approaching the end of the free surface. However, σ_3/σ_1 of butterfly-type joints decreases rapidly with increasing distance from the free end.
(4) The maximum principal, the von Mises equivalent and the maximum shear stresses are not adequate as criteria for estimating endurance limits of these adhesive joints.
(5) The maximum principal, the von Mises equivalent and the maximum shear stresses in the uniform stress region at the endurance limit decrease linearly with the increase of the principal stress ratio, σ_3/σ_1. Furthermore, the von Mises equivalent and the maximum shear stresses at the endurance limit are more sensitive to the principal stress ratio than the maximum principal stress; however, the experimental equations based on the Von Mises equivalent and the maximum shear stresses enable us to estimate endurance limit with a little higher accuracy than that based on the maximum principal stress.

Acknowledgements

This work was partly supported by a Grant-in-Aid for Scientific Research C (No. 04650086), from the Ministry of Education, Science and Culture, Japan in the fiscal year of 1992 and 1993.

References

1. L. J. Lubkin *J. Appl. Mech.* **24**, 255 (1957).
2. Y. Suzuki *J. Adhesion Soc. Japan* (in Japanese) **18**, 7 (1982).
3. Y. Suzuki *Bull. JSME* **28**, 2575 (1985).
4. Y. Suzuki *JSME Inter.* **30**, 1042 (1987).
5. D. W. Adkins and R. B. Pipes *Comp. Sci. Tech.* **22**, 209 (1985).
6. H. Kyogoku, T. Sugibayashi, K. Ikegami, *Trans. Jpn. Soc. Mech. Eng. Ser. A* (in Japanese) **53**, 499 (1987).
7. N. Goldenberg, M. Arcan and E. Nicolau **ASTM STP 247**, 115 (1958).

8. L. Banks-Silla and M. Arcan, **ASTCM STP 905**, 347 (1986).
9. V. Weissberg and M. Arcan, **ASTM STP 981**, 28 (1988).
10. L. Banks-Silla and D. Sherman, *Int. J. Fract.* **50**, 15 (1991).
11. K. M. Liechti and T. Hayashi, *J. Adhesion*, **29**, 167 (1989).
12. For example, Y. Narusawa, *Strength of Polymeric Materials* (in Japanese) (Oumu Sha, Tokyo, 1982).